

PAPER • OPEN ACCESS

## Fundamental mode intensity evolution in tapered optical fibres

To cite this article: J R Ek-Ek *et al* 2020 *Laser Phys.* **30** 126204

View the [article online](#) for updates and enhancements.

# Fundamental mode intensity evolution in tapered optical fibres

J R Ek-Ek<sup>1</sup>, F Martinez-Pinon<sup>1</sup>, J A Alvarez-Chavez<sup>2</sup>, D E Ceballos-Herrera<sup>3</sup>, R Sanchez-Lara<sup>4</sup> and H L Offerhaus<sup>2</sup>

<sup>1</sup> Instituto Politecnico Nacional - Centro de Investigacion e Innovacion Tecnologica, Mexico

<sup>2</sup> Optical Sciences Group - University of Twente, Drienerlolaan 5, 7522 NB, Enschede, The Netherlands

<sup>3</sup> Instituto de Ingenieria, Universidad Nacional Autonoma de Mexico (UNAM), Cd. Universitaria, Alcatla Coyoacan, 04510, Ciudad de Mexico, Mexico

<sup>4</sup> Facultad de Ingenieria, Universidad Autonoma del Carmen, Ciudad del Carmen, Campeche, Mexico

E-mail: [j.a.alvarez-chavez@utwente.nl](mailto:j.a.alvarez-chavez@utwente.nl)

Received 8 April 2020

Accepted for publication 24 September 2020

Published 19 November 2020



CrossMark

## Abstract

The mode field intensity, spot size, central peak intensity evolution and adiabaticity are calculated for different points along the transition of an optical fibre taper that adiabatically tapers from the standard 125 nm down to 1  $\mu\text{m}$  and then to 440 nm diameter for low loss operation at 1550 nm wavelength. The first section of the taper is evaluated using a weak guidance approximation. The second section is treated as a three-index layer structure (double-clad) and evaluated with eigenvalue equations for three refractive indices. The third and thinnest section of the taper is studied using an exact mode eigenvalue equation. The results show that the fundamental mode for the third section has a discontinuity at the fibre edge with a peak intensity larger than the intensity at the centre of the fibre. Since the guiding by the core disappears in the first section of the taper, the mode field does not simply reduce monotonously along the taper with the outer diameter of the fibre. By this novel approach, and for the first time, to the best of our knowledge, the taper shape that complies with the adiabaticity criterion, the mode intensity profile and the spot size (first Petermann definition) of the fundamental mode evolution, along their position on the taper are determined.

Keywords: optical fibres taper, fundamental mode evolution, spot size evolution, adiabaticity condition, first Petermann definition

(Some figures may appear in colour only in the online journal)

## 1. Introduction

It is almost five decades since tapers in optical fibres were identified as a significant topic of research [1]. Tapered fibres are enjoying renewed interest because of useful applications as optical fibre sensors and couplers [2]. Examples of these are evanescent wave biosensors [3–6], hydrogen detection [7], astro-photonics devices [8, 9], fibre optic laser applications

[10, 11], chemical pollutants detection in seawater [12] also [13]. The analysis of fibre tapers including the adiabatic concept, has been available since 1983 in a textbook and papers [14, 15]. The concept of adiabaticity states that it is possible to fabricate low loss tapers provided that their geometrical shape varies slowly, so it does not allow energy conversion from the fundamental mode (LP<sub>01</sub> or HE<sub>11</sub>) to the next circularly symmetric mode (LP<sub>02</sub> or HE<sub>12</sub>). This can also be applied to single mode fibre tapers. In 2003, a new development was reported: that the fibre taper waist diameter can be downsized to 1  $\mu\text{m}$  (micro optical fibre) or even less (approximately down to 200 nm) in what was called ‘sub-wavelength diameter silica wires’ [16]. Some authors refer to these ultra-thin optical fibres as ‘nano optical fibres’. In this work, the



Original content from this work may be used under the terms of the [Creative Commons Attribution 3.0 licence](https://creativecommons.org/licenses/by/3.0/). Any further distribution of this work must maintain attribution to the author(s) and the title of the work, journal citation and DOI.

term ‘sub-micro’, which we believe is more accurate, is used. The significance of this result was that these fibre devices can have new optical properties and new applications as depicted in the ‘Tong Tree’ [16]. This has been called ‘The second life of optical fibre tapers’ [17] as its technology entered a very productive phase. However, little detailed attention has been paid to the evolution of the fundamental mode intensity and its exact shape distribution along all the fibre, from the standard size (125 μm) to the micro size (1 μm) and sub-micro size (200 nm).

The core diameter for standard fibres is approximately 8 μm for an SMF-28 Corning optical fibre at 125 micron outer diameter. This core shrinks to 64 nm at 1 μm external diameter and less than 15 nm at 220 nm external diameter. If we consider that the guiding limit is around 200 nm [18], the original core effectively vanishes at microscopic and sub-microscopic sizes and a new optical waveguide is formed by the cladding and the surrounding medium. Analysis of the mode therefore requires the evaluation of the eigenvalue equation at many successive points along the taper for the general case of a three-layer refractive index profile waveguide. As the mode intensity profile extends beyond the core, the peak amplitude decreases, preserving the total amount of optical power in the fundamental mode. It is critical to observe how the mode intensity changes along the tapered fibre. The results show novel, unexpected variations in the mode intensity profile and spot size along the taper. The application of the adiabatic criterion yields unexpectedly long tapers.

The analysis starts by assuming an initial hypothetical shape based on an experimental taper reported by Linslal [19, 20]. The proposed theoretical taper shape is shown in figure 1, subdivided to include a section which is ‘micro’, i.e. 1 μm waist diameter and another section which is ‘sub-micro’ or ‘sub-wavelength’ with a minimum waist diameter of 440 nm at 1550 nm wavelength. A diameter smaller than 200 nm reaches the guiding limit and the waveguide effect ceases to exist at a wavelength of 633 nm. The taper has been assumed to be a symmetric biconical shape with 19 equidistant points (identified by the letters A-S, 2 mm apart) along the taper from the initial standard size A (125 μm diameter) to the smallest waist diameter at S (440 nm). As the taper is symmetric, the waveguide parameters in the tapering down section (A-S) are mirrored in the tapering up section (S-A). The shape of the taper was divided into three sections: section 1 (from point A to F), section 2 (from point G to N) and section 3 (from point O to S).

The first section has two refractive indices corresponding to a single mode (at 1550 nm) with an initial cladding radius of 62.5 μm and an initial core radius  $a(0) = 4 \mu\text{m}$ . The refractive indices of the core and cladding are  $n_1 = 1.46125$  and  $n_2 = 1.45625$  respectively. The second section has three refractive indices  $n_1, n_2, n_3$  and a core radius ‘a’ and a cladding radius ‘b’.  $n_1$  and  $n_2$  are the same as in the first section, and  $n_3 = 1.0$  (air) [21]. In the third section, the core has become so small that it has effectively disappeared and only two refractive indices  $n_2 = 1.46125$  and  $n_3 = 1.0$  remain. The fibre radius goes from 611 nm (O point) to 220 nm (S point).

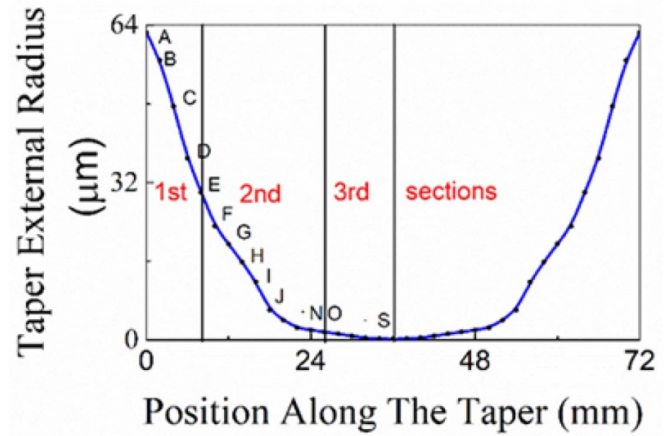


**Figure 1.** Initial theoretical taper shape. Length = 72 mm, Initial external diameter (A) = 125 μm, Taper waist (at S) = 0.44 μm.

## 2. Eigenvalue equations for the fundamental mode propagation

To determine the mode intensity profile evolution along the taper, the solution of three different sets of eigenvalue equations is required. For points A to E, the weakly guiding mode equation is employed [22].

$$u \frac{J_{\nu+1}(u)}{J_{\nu}(u)} = w \frac{K_{\nu+1}(w)}{K_{\nu}(w)} \quad (1)$$

Where ‘u’ and ‘w’ are the modal parameters as defined as:  $u = a(k_0^2 n_1^2 - \beta^2)^{1/2}$ ,  $w = a(\beta^2 - k_0^2 n_2^2)^{1/2}$ ,  $a$  = core radius,  $k_0 = 2\pi/\lambda$ ,  $\beta$  is the mode propagation constant.  $J_{\nu}$  is the Bessel function of the first kind of order  $\nu$ ,  $K_{\nu}$  is the modified Bessel function of the second kind of order  $\nu$ .

From points F to N, the Monerie equation is used [23] and for the last section (points M to S) the exact mode equation is employed [14] as:

$$\left( \frac{J'_1(u)}{uJ_1(u)} + \frac{K'_1(w)}{wK_1(w)} \right) \left( \frac{J'_1(u)}{uJ_1(u)} + \frac{n_3^2 K'_1(w)}{n_2^2 wK_1(w)} \right) = \left( \frac{\beta}{kn_2} \right)^2 \left( \frac{V}{UW} \right)^4 \quad (2)$$

## 3. Results and discussion

The intensity profiles for points A to F are shown in figure 2. Note how the wings start to rise from point E onwards.

For the second section the results are shown in figure 3 below.

Note how the mode expands considerably in the first part of the third section, where it moves outside the core and into the cladding, only to contract again in the second part. For the final section the results are shown in figure 4. Here again the mode expands as it loses guiding by the cladding, but now the surrounding air has a much lower refractive index, so that the mode remains close to the remaining fibre.

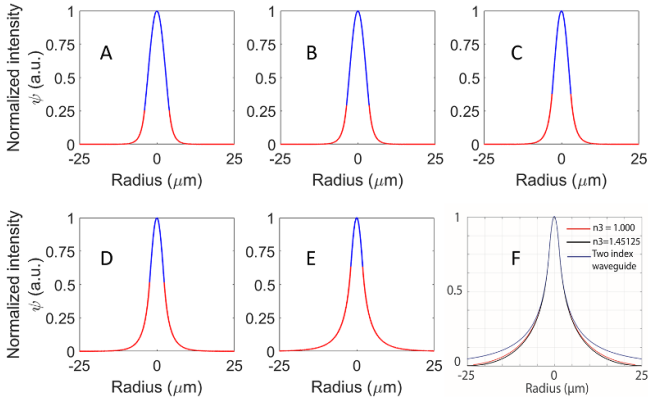


Figure 2. Fundamental mode intensity from points A to F.

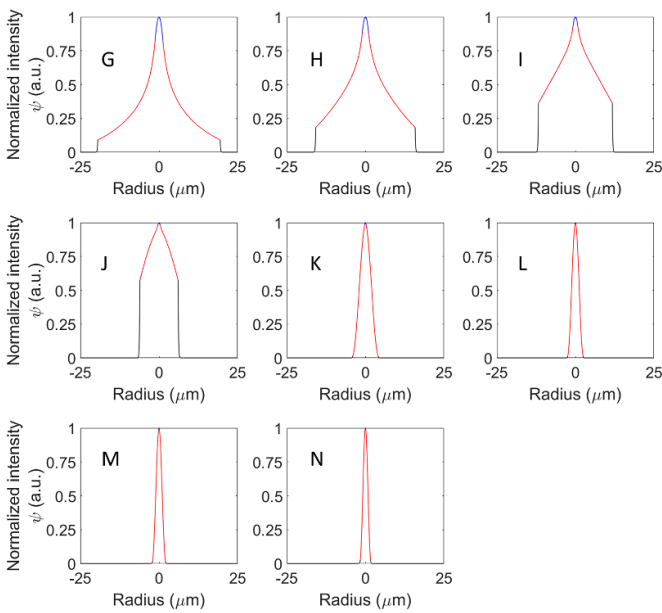


Figure 3. Fundamental mode intensity from points G to N.

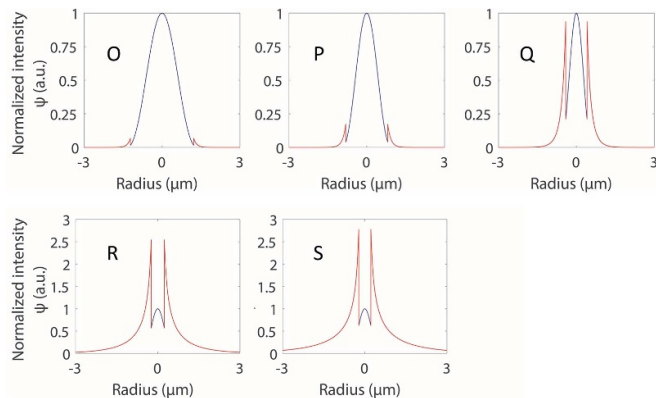


Figure 4. Fundamental mode intensity from points O to S.

### 3.1. Adiabaticity criterion

For most applications, it is important to ensure that the optical fibre taper is adiabatic so that the taper represents low optical

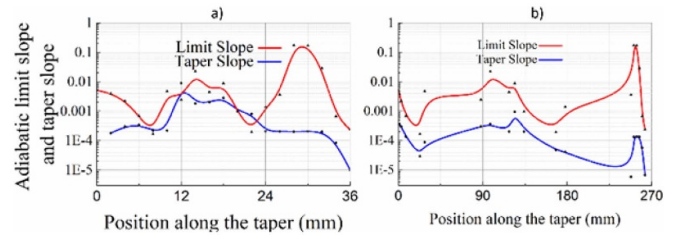


Figure 5. (a) Limit slope given by the adiabatic criterion and the (b) adjusted taper slope for low optical loss.

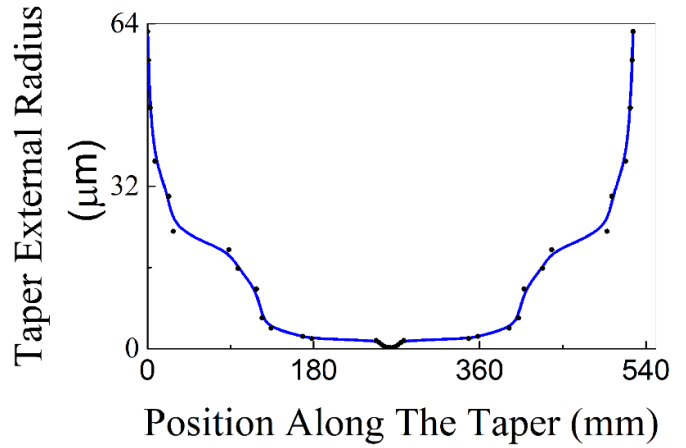


Figure 6. Designed taper geometry to meet the adiabatic criteria (overall biconical taper length).

losses [14]. Figure 5 shows the adiabatic limit slope versus taper slope as expressed by the following equation:

$$\left| \frac{da(z)}{dz} \right| \ll \left| \frac{a(z)}{z_b} \right| \quad (3)$$

$$z_b = \frac{2\pi}{\beta_1 - \beta_2} \quad (4)$$

Where  $a(z)$  is the effective core radius of the waveguide (in some cases is  $b(z)$ ),  $z_b$  is the beat length between the  $LP_{01}$  and  $LP_{02}$  modes (or  $HE_{11}$  and  $HE_{12}$  modes),  $\beta_1$  is the propagation constant of  $LP_{01}$  (or  $HE_{11}$  mode) and  $\beta_2$  is the propagation constant of  $LP_{02}$  (or  $HE_{12}$  mode). The rate of change of the taper (taper slope) should be lower than the rate of change given by the theoretical limit slope which is a function of the effective core radius of the fibre divided by the beat length of the first circular symmetric modes. It should be noted that when the taper is single mode,  $\beta_2$  corresponds to the cut-off condition of the  $LP_{02}$  mode equal to  $n_2k_0$  or  $n_3k_0$ .

Using the adiabatic limit slope, the initial taper shape of figure 1 was modified to ensure adiabaticity. Figure 5 shows the adiabatic limit slope.

The main consequence is that the overall taper length is now quite large: 526 mm (figure 6). Also, the shape of the outside diameter is no longer monotonous but reflects the fact that the mode first ‘escapes’ the confinement by the core and later loses the guidance by the cladding.

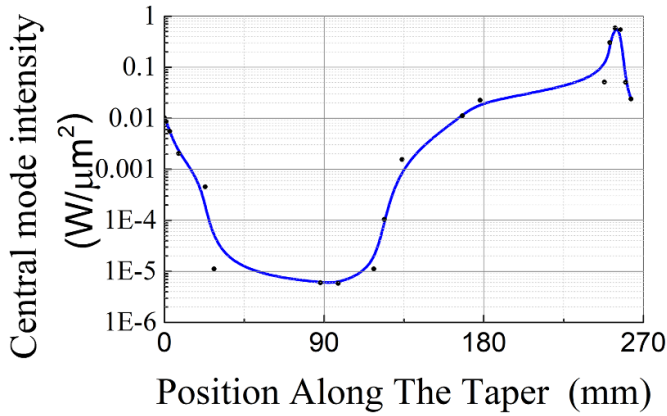


Figure 7. Central mode intensity evolution along the tapered fibre.

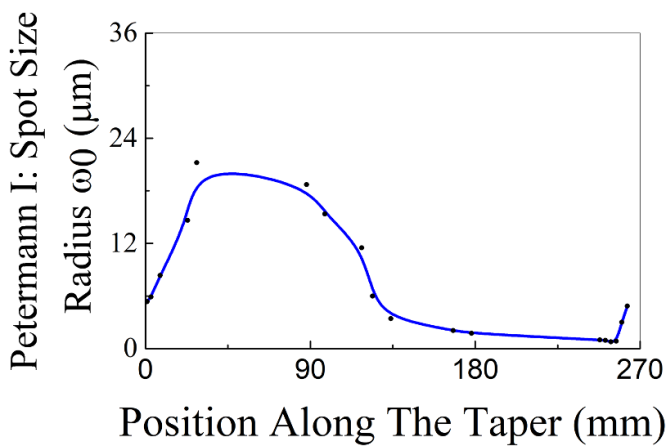


Figure 8. Spot size evolution along the tapered fibre.

### 3.2. Fundamental mode field intensity evolution

Figure 7 shows the evolution of the central mode intensity on the axis along the tapered fibre. It is calculated assuming that the optical power launched at point A is 1 Watt. The normalisation is shown in equation (5) and determines the coefficient  $A_0$ . The units for the intensity profile are in Watts per squared micrometre, as micrometre units for the radial coordinate  $r$  are being used in this work.

$$P = 2\pi \int_0^\infty [A_0\varphi]^2 r dr = 1 \text{ Watt} \quad (5)$$

Given the adiabaticity, all profiles calculated along the length (B-S) can be normalized in the same way. Figure 7 shows  $A_0$  as a function of the position along the taper. It can be seen that the central mode intensity decreases as the field initially expands away from the core and subsequently increases as the cladding start to confine the field again.

To show how the spot size radius ( $\omega_0$ ) changes along the taper, we use the first Petermann definition as given by equation (6):

$$\omega_0 = \sqrt{2 \left[ \frac{\int_0^\infty \varphi^2(r) r^3 dr}{\int_0^\infty \varphi^2(r) r dr} \right]^{1/2}} \quad (6)$$

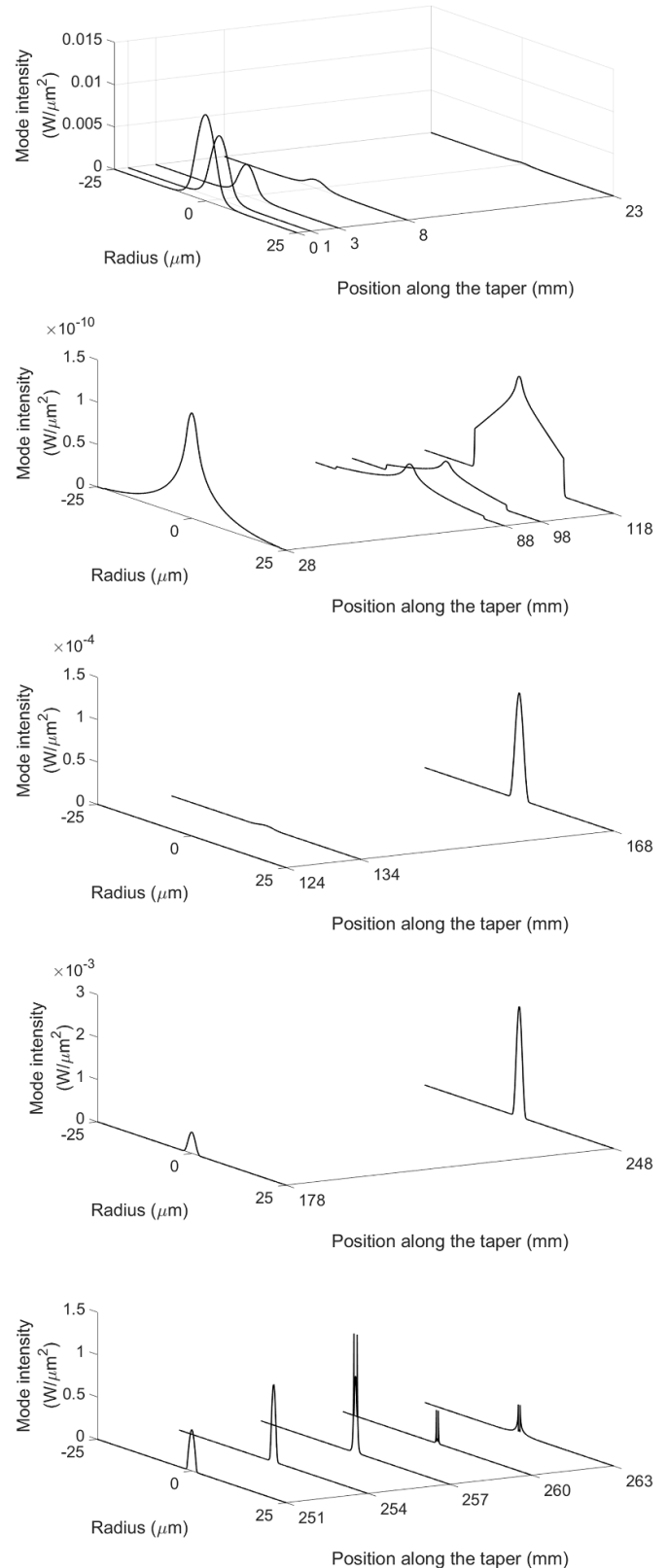


Figure 9. Mode intensity profile along the tapered fibre.

Where  $\varphi$  is the fundamental mode field. The spot size directly shows the expansion and contraction of the mode field, and therefore evolves inversely to the field intensity profile. In this work, the spot size definition for the Gaussian

approximation for the mode field is not used as it does not apply for the majority of points along the taper. Figure 8 shows the spot size evolution along the position of the taper.

The spot size radius increases in the first section of the taper, reaching a maximum (21.20  $\mu\text{m}$ ) at point F with 23.13  $\mu\text{m}$  of fibre external radius, showing the mode expands to fill the cladding. Subsequently the spot size evolution follows the outer radius down to (0.76  $\mu\text{m}$ ) at point P for 0.81  $\mu\text{m}$  of fibre external radius. The spot size radius then increases again to 4.84  $\mu\text{m}$  as the 220 nm of fibre external radius no longer effectively confines the mode.

### 3.3. Mode intensity profile evolution

The detailed mode intensity profiles can be presented only using different logarithmic scales as the variation is very large. Figure 9 shows how the mode intensity profiles increases at the end of the taper with respect to the initial mode intensity at the beginning of the taper in a linear scale only the last five profiles can be shown.

It can be seen that the central mode intensity is nearly 58 times larger at the submicron size (0.81  $\mu\text{m}$  of fibre external radius) as compared with the initial standard size of the taper. For comparison, the thinning of the taper is 77 times. It is important to realize that the smallest spot size is not at the thinnest end of the taper. Also, it must be kept in mind that the peak intensity of the profile at the thin end is at the edge of the fibre, the maximum being at point Q, for this case the ratio of this edge mode intensity to the central mode intensity of point A is approximately 80 times, which again can be very useful for submicron optical fibre sensors and devices.

## 4. Conclusion

This work has presented a novel but realistic simulation of the evolution of the mode intensity profile along a tapered fibre, from standard size (125  $\mu\text{m}$  external diameter) to micron and submicron size external diameter, with 440 nm being the smallest waist size operating at 1550 nm wavelength for the case of a taper in air. The first section was evaluated via the weak guidance approximation. The second section was treated as a three-index layer structure and evaluated using eigenvalue equations for three refractive indices. The third and thinnest section of the taper was studied using an exact mode eigenvalue equation. With this rigorous strategy, optimum fibre external diameter values for smallest spot sizes and largest mode field intensities were found, suitable for low-loss taper applications. It is expected that this analysis will be useful for researchers in the area of evanescent submicron optical fibre sensors.

## Acknowledgments

The authors would like to thank IPN, IPN-CIITEC, UNAM, UNACAR and CONACYT from Mexico and the Optical

Sciences group at the University of Twente in the Netherlands for financing their projects and scholarships.

## References

- [1] Snyder A W 1970. Coupling of modes on a tapered dielectric cylinder *IEEE Trans. Microw. Theory Tech.* **7** 383–92
- [2] Li H, Li S, Yang T, Xu J, Li J, Chen W, Wang P, Dai T, Wang G and Yang J 2019 Silicon two-mode multi/demultiplexer based on tapered couplers *Optik - Int. J. Light Electron Opt.* **176** 518–22
- [3] Wiejata J P, Shankar P M and Mutharasan R 2003 Fluorescent sensing using biconical tapers *Sci. Direct* **96** 315–20
- [4] Zhang Z et al 2014 A double-taper optical fiber-based radiation wave other than evanescent wave in all-fiber immunofluorescence biosensor for quantitative detection of escherichia coli *PLoS ONE* **9** O157:H7
- [5] Descamps E, Duroure N, Deiss F, Thierry Leichle C, Mailley A P, Ait-Ikhlef A, Livache T, Nicu L and Sojic N 2013 Functionalization of optical nanotip arrays with an electrochemical microcantilever for multiplexed DNA detection *R. Soc. Chem.* **13** 2956–62
- [6] Loyez M, Ribaut C, Caucheteur C and Wattiez R 2019 Functionalized gold electroless-plated optical fiber gratings for reliable surface biosensing *Sensors Actuators B* **280** 54–61
- [7] Villatoro J and Monzon-Hernandez D 2005 Fast detection of hydrogen with nano fiber tapers coated with ultra-thin palladium layers *Opt. Express* **13** 5087–92
- [8] Bland-Hawthorn J and Kern P 2009 Astrophotonics: a new era for astronomical instruments *Opt. Express* **17** 1880–4
- [9] Benitez-Alvarez R, Martinez-Pinon F and Orlov V G 2019 A new method for actively tuning FBG's to particular infrared wavelengths for OH emission lines suppression *Revista Mexicana de Astronomia y Astrofisica* **55** 351–61
- [10] Cong X, Huang Y, Zhang M, Su H, Li I L and Liang H 2018 Graphene-coated nanowires with dropshaped cross section for the low loss propagation of THz waves with sub-micron mode widths *Laser Phys. Lett.* **15** 096001
- [11] Khudyakov M M et al 2019 Single-mode large-mode-area Er–Yb fibers with core based on phosphorosilicate glass highly doped with fluorine *Laser Phys. Lett.* **16** 025105
- [12] Irigoyen M, Sánchez-Martin J A, Bernabeu E and Zamora A 2017 Tapered optical fiber sensor for chemical pollutants detection in seawater *Meas. Sci. Technol.* **28** 045802
- [13] Saleh N M and Aziz A A 2018 Simulation of surface plasmon resonance on different size of a single gold nanoparticle *J. Phys.: Conf. Ser.* **1083** 012041
- [14] Snyder A W and Love J D 1983 *Optical Waveguide Theory* (London: Chapman and Hall)
- [15] Love J D, Henry W M, Stewart W J, Black R J, Lacroix S and Gonthier F 1991 Tapered single-mode fibers and devices. I. Adiabaticity criteria *IEE Proc. J - Optoelectron.* **138** 343–54
- [16] Tong L M, Gattas R R, Ashcom J B, He S L, Lou J Y, Shen M Y, Maxwell I and Mazur E 2003 Subwavelength-diameter silica wires for low-loss optical wave guiding *Nature* **426** 816–9
- [17] Brambilla G 2012. The second life of optical fiber tapers XXXV Encuentro Nacional de Física de la Materia Condensada, Brazil
- [18] Sumetsky M 2013 Nanophotonics of optical fibers *Nanophotonics* **2** 393–406
- [19] Birks T A and Li Y W 1992 The shape of fiber tapers *J. Lightwave Technol.* **10** 432–8
- [20] Linslal C L, Mohan P M, Halder A and Gangopadhyay T K 2012 Eigenvalue equation and core-mode cutoff of weakly

- guiding tapered fiber as three layer optical waveguide and used as biochemical sensor *Appl. Opt.* **51** 3445–52
- [21] Mathar R J 2007 Refractive index of humid air in the infrared: model fits *J. Opt. A: Pure Appl. Opt.* **9** 470–6
- [22] Gloge D 1971 Weakly guiding fibers *Appl. Opt.* **10** 2252–8
- [23] Monerie M 1982 Propagation in doubly clad single-mode fibers *IEEE J. Quantum. Electron.* **18** 535–42